Revista Brasileira de Meteorologia, v.17, n.2, 125-140, 2002

A FIRST-GUESS FIELD PRODUCED BY MERGING DIGITAL FILTER AND NUDGING TECHNIQUES[1]

VALDIR INNOCENTINI[2], ERNESTO CAETANO[3] AND FABRICIO PEREIRA HARTER[2]

[2] Instituto Nacional de Pequisas Espaciais, MCT, São José dos Campos, Brasil
[3] Centro de Ciencias de la Atmósfera, UNAM
Av. Circuito Exterior s/n, Ciudad Universitaria 04510, México D.F., México
caetano@servidor.unam.mx

ABSTRACT

A method combining the nudging and digital filter techniques is proposed to obtain the first-guess for a limited area model (LAM). The method consists on the integrate the LAM model starting with a previous run valid at 6 hours before the first-guess target time, over a 12 hours period applying the filter, and nudging, only on the first 6 hours span, an analysis valid at the target time produced by a global model. The boundary conditions are also provided by the same global model. The advantages of the method are i) the prognostic fields given by the LAM are corrected by the global analysis consistent with the boundary conditions, and ii) it makes the initialization.

Tests with a simple gravity wave model reveal the Gibbs phenomenon, which is well controlled by the Lanczos window in an initialization by digital filter, enhancing with the proposed method. Whereas this shortcoming occurs mainly at shorter waves, it can be reduced by horizontal diffusion. The method is implemented in a LAM and the results indicated that the scheme is efficient, cheap, and the Gibbs phenomenon seems to have been successfully controlled by the numerical artifices usually implemented in a LAM, with no need for further dumping. The two advantages mentioned above are achieved.

Key words: atmospheric modelling, data assimilation, initial conditions

RESUMO: CONDIÇÕES INICIAIS PRODUZIDAS PELA COMBINAÇÃO DE FILTRO DIGITAL E RELAXAÇÃO DE DADOS

Uma metodologia combinando filtro digital relaxação newtoniana é proposta para obter condições iniciais para um modelo de área limitada (LAM). O método consiste em integrar o modelo LAM por um período de 12 horas, iniciando 6 horas antes da hora da condição inicial, aplicando o filtro digital durante todo período, e a relaxação apenas nas primeiras 6 horas. Os dados assimilados na relaxação são da analise global de um modelo global no horário que a condição inicial é desejada. A condição de fronteira é fornecida pelo mesmo modelo global. As vantagens do método são i) os campos prognósticos obtidos pelo LAM são corrigidos pela análise global consistente com as condições de fronteiras, e ii) fornece a inicialização.

Testes com um modelo simplificado de ondas de gravidade mostra que os fenômeno de Gibbs, que é bem controlado pela janela de Lanczos em uma inicialização por filtro digital, é enaltecido no presente método. Devido a este problema ocorrer apenas em ondas curtas, acredita-se que possa ser controlado eficientemente por difusão horizontal. O método é aplicado em um LAM e mostra que o esquema é eficiente, utiliza pouco tempo computacional, e o fenômeno de Gibbs é, de fato, controlado pelos artificios numéricos usualmente implementados em um LAM, sem necessidade de adicionais amortecimentos. As duas vantagens apontadas acima foram alcançadas no experimento com LAM.

Palavras-chaves: modelagem atmosférica, assimilação de dados, condições iniciais

1. INTRODUCTION

The use of initial conditions provided by an objective analysis without any previous adjustment can rise the excitation of high-frequencies gravity waves with amplitudes not observed in the atmosphere. These noises are noticeable mainly during the first hours of a numerical integration. Although they can be dumped by numerical

[1] Submetido em setembro/2001; aceito em maio/2002

artifices, the model outputs have limited utility during the adjustment period. Also the dumping can be harmful to the meteorological waves. Initialization schemes devised to avoid inconsistency between initial condition and the model equations, or imbalances between the mass and wind fields, aim to suppress high-frequency modes in the initial field, responsible for strong mass convergence/ divergence.

An approach widely employed in global models is the nonlinear normal mode initialization (NNMI) introduced by Baer and Tribbia (1977) and Machenhauer (1977). A review of this method is given by Daley (1981). Limited area models offer some analytical difficulties in the use of this technique, and an attractive alternative is the Digital Filter (DF), suggested by Lynch and Huang (1993) and Gustafsson (1992). The method was successfully implemented in the HIRLAM (High-Resolution Limited-Area Model), producing equivalent or better results than the NNMI (HUANG and LYNCH 1993).

The mathematical formulation of the method consists on to obtain a filtered value from a linear combination of a sequence using symmetric weights. The result substitutes the sequence by only one centered value. The application of the method on a set of sequences yields a new filtered sequence. Contrasting with the theoretical characteristic of the filter, which provides a new temporal sequence free of high frequencies, in a numerical model, supposing the initial time is 00Z and the filter is applied in a 12-h period of integration, the filtered initial condition refers to the time 06Z; no new time sequence is produced, but only a single value at each grid-point. One should enquire where is the information that the undesirable frequencies were cut off. Although Lynch and Huang (1992) have shown effectiveness of DF in the initialization, it may be argued that the result seems rather pragmatic. Certainly the information that some frequencies were cut off from the filtered initial condition must have been transported to the spatial scale, but this is not clear in a first view.

Fillion et al. (1995) extended the DF to a global data assimilation system. They refer to the filtered field as DF finalization, obtained by a 12-h forward integration. The time series generated give a filtered analysis valid at 6-h into the integration. This field constitutes the background condition (or first-guess) for the next analysis employing three or four-dimensional variational data assimilation schemes. In this kind of data assimilation a higher-order balance constraint can be incorporated eliminating the needs for an initialization procedure, but in general operational statistical analysis scheme gives place to large amplitude unrealistic gravity wave.

The DF proposed by Lynch and Huang (1993) mentioned above integrates the model diabatically forward and adiatabically backward obtaining the initial condition at 0-h into the integration, while Fillion et al. (1995) proposed to integrate the model only forward resulting in a first-guess at 6-h.

Limited area numerical models (LAM) use the initial and boundary conditions provided by a larger area model, usually a global model (GM). In general, the grid of both models is different, requiring a spatial interpolation to the LAM grid. This procedure causes a large unbalance between mass and wind fields, which demands the application of an initialization technique. Since the DF is an easy method for the initialization, there are two possibilities. First is to integrate the model forward and to obtain the initial condition 6-h after the GM initial condition time (as in FILLION et. al 1995); and second is to integrate the model adiabatically backward and diabatically forward to obtain the initial condition or first-guess at 0h. An alternative approach however, which will be examined in this work, is to start the LAM integration 6 hours earlier than the GM analysis. Then apply the DF for a 12 hours integrating period from an initial condition given by a previous LAM run. Furthermore the prognostic variables are modified by the GM analysis using a nudging technique during the integration. Such procedure has the advantage of avoiding the needs of integrating the model adiabatically backwards and also the initial condition takes into account to the global analysis of that time as well as the trend of a previous LAM prediction.

Due to its simplicity, the nudging technique (Hoke and Anthes 1976) has been largely employed to introduce the observational data into a model output. The method consists in to add an extra term into the prognostic model equations, whose value depends on the observational time and distance from the grid-point. More recently operational centers have used more robust methods based on variational analysis, which demand additional computational time. As a general rule, the nudging term must be much smaller than the other terms of the prognostic equation, and most of the users conclusions of this method are based on pragmatic results from numerical experiments. For example, Kuo et al. (1993) concludes that nudging winds produces better results than nudging temperature alone, and nudging both fields can produce worse results than the wind alone.

The main objective of this research is to examine the feasibility of the alternative idea designed above for

initialization, combining the DF and the nudging techniques to generate a filtered first-guess valid at the time of a assimilated GM analysis. Section 2 presents a brief theoretical formulation of the two methods. In Section 3 a simple linear gravity-wave numerical model is proposed, and the effectiveness of DF is examined in this simple model employing the harmonic analysis tool to detect the spatial modes being cut off. Section 3 also applies the nudging technique to the simple model with the objective to know how the model responds to the nudging weight, and to the assimilation of only one or two prognostic variables. The approach combining both methods is implemented in a primitive equation limited area numerical model and presented in Section 4. The results are discussed in a simulation of a cyclone development over the South Atlantic, using the analysis provided by the NCEP reanalysis. Finally, the main results are summarized in Section 5.

2. THEORETICAL FRAMEWORK

A brief description of Digital Filter (DF) and nudging (or Newtonian) techniques are presented.

a. The digital filter

The formulation of the DF as used in meteorology can be found in several works (e. g. Lynch and Huang 1992; Fillion et al. 1995; Doblas-Reyes and Dèque 1998). It is a low-pass non-recursive filter and can be implemented easily in a numerical model without considerable additional computational efforts.

Consider a sequence $\{f_n\}$ and its Fourier Transform

$$f_n = \frac{1}{2\pi}\int_{-\pi}^{\pi} F(\omega)e^{i\omega n}\,d\omega \qquad 2.1\text{ - a}$$

$$F(\omega) = \sum_{n=-\infty}^{\infty} f_n e^{-i\omega n} \qquad 2.1\text{ - b}$$

By defining the function of the frequency ω

$$H(\omega) = \begin{cases} 1, & if \quad |\omega| \le |\omega_c| \\ 0, & otherwise \end{cases} \qquad 2.2$$

where ω_c is the cutoff frequency, it follows that the product

$$F(\omega)H(\omega) \qquad 2.3$$

retains only frequencies greater then ω_c. The filtered sequence $\{f_n^*\}$ is constituted by elements in the form:

$$f_n^* = \frac{1}{2\pi}\int_{-\pi}^{\pi} F(\omega)H(\omega)e^{int}\,d\omega \qquad 2.4$$

where t is the time.

The use of the convolution theorem allows obtaining the filtered sequence without computing the integral (2.4). Given two sequences $\{f_n\}$ and $\{h_n\}$, the convolution is defined by

$$(h * f)(n) = \sum_{k=-\infty}^{\infty} h_k f_{(n-k)} \qquad 2.5$$

where n and k are integer numbers. The theorem of convolution establishes that

$$H(\omega)F(\omega) = \sum_{k=-\infty}^{\infty}(h * f)(k)e^{-i\omega k} \qquad 2.6$$

Then, the filtered sequence given by (2.4) has the form

$$f_n^* = \frac{1}{2\pi}\int_{-\pi}^{\pi}\left[\sum_{k=-\infty}^{\infty}(h * f)(k)e^{-i\omega k}\right]e^{i\omega n}\,d\omega$$

which is reduced, due to the ortogonality relations to

$$f_n^* = (h * f)(n) \qquad 2.7$$

The Fourier transform of the sequence $\{h_n\}$, defined below, is

$$h_n = \frac{1}{2\pi}\int_{-\pi}^{\pi} H(\omega)e^{i\omega n}\,d\omega = \frac{1}{2\pi}\int_{-\omega_c}^{+\omega_c} e^{i\omega n}\,d\omega = \frac{sen(n\omega_c)}{n\pi}$$

Therefore, according to (2.7), one element of the filtered sequence $\{f_n^*\}$ is

$$f_n^* = \sum_{k=-\infty}^{\infty} \frac{\text{sen}(k\omega_c)}{k\pi} f_{n-k}$$

In practical problems, the digital filter is used in a finite sequence. This introduces the Gibbs oscillations near the cutoff frequency ω_c. Several windows have been proposed to solve this problem, resulting in a new filtered sequence with 2N+1 elements given by

$$f_n^* = \sum_{k=-N}^{k=+N} \frac{sen(k\omega_c)}{k\pi} f_{(n-k)} \sigma(k,N) \qquad 2.8$$

where $\sigma(N,k)$ is the controlling factor of the Gibbs phenomenon. A common window, according to Hamming (1989), is the Lanczos window, defined by

$$\sigma(k,N) = \frac{sen(k\pi/N)}{k\pi/N} \qquad 2.9$$

b. The nudging method

The nudging method consists in relaxing the value of a variable towards the observation during the model integration by adding a tendency term in its prognostic equation. The nudging is controlled by the specification of parameters depending on the time and space separations between the observation and model at each grid-point and time-step. In most applications, the parameter value must take account of the data quality and its representativeness, which is not the case of the present study.

For a generic prognostic variable u, its equation takes the form

$$\frac{\partial u}{\partial t} = F(u) + GW(u_{ana} - u)$$

where F represents the physical processes and the last term is the artificial forcing. The nudging term depends on the difference between the observed and forecasted value of u. It tends to increase (decrease) u when $u_{ana} < u$ ($u_{ana} > u$). The factor G is named nudging coefficient. The weight function W is decomposed into its horizontal, temporal and vertical components:

$$W = W_{xy} W_t W_z$$

The weight components consider the influence of use $u_{ana} - u$ at locations and times whose distance to the actual grid-point and time-step model are less than a prescribed radius of influence R and a time window 2T. In this research the analysis is interpolated to the grid-points, and the spatial weight is 1 at the grid-point corresponding to the analysis location, and null otherwise. The temporal weight function assumes the trapezoidal form:

$$W_t = \begin{cases} 1 & |t_{ana} - t| \le \frac{T}{2} \\ 0 & |t_{ana} - t| \ge T \\ 2\left[T - |t_{ana} - t|\right] & \frac{T}{2} < |t_{ana} - t| < T \end{cases} \qquad 2.10$$

where t is the model time and t_{ana} is the time of the analysis to be nudged.

3. APPLICATION TO A SIMPLE GRAVITY WAVE MODEL

The purpose of this section is to implement the ideas delineated above in a simple model so that the results can be better understood. The model proposed is numerically unstable so that no solution is dumped by other reason than the filter. The effect of the DF, nudging, and both together on the frequencies and spatial modes are examined and discussed before its implementation on a complex meteorological model.

a. The simple model

In an effort to extract information about the properties of the proposed method, a simple set of equations with known solutions will be considered. A well-known problem is the simplified shallow water model given by

$$\frac{\partial u}{\partial t} = -\frac{\partial \phi}{\partial x} \qquad 3.1\text{-a}$$

$$\frac{\partial \phi}{\partial t} = -c^2 \frac{\partial u}{\partial x} \qquad 3.1\text{-b}$$

where u is the velocity along the axis x, t is the time $c = \sqrt{gH}$ and h is the perturbation of the geopotential height from a basic height H. These equations are often used to test and to illustrate numerical methods, since their solutions are the fast-moving gravity waves, which usually bring difficulties in to integrate the atmosphere governing equations. In an infinite cyclic domain, supposing an initial condition $F(x)$, the solution is composed by two conservative signals propagating to the left and to the right of the axis x with phase velocity c, that is

$$\tfrac{1}{2}\left[F(x+ct) + F(x-ct)\right]$$

A combination between (3.1-a) and (3.1-b) yields the energy equation

$$\frac{\partial}{\partial t}\left(\frac{u^2 + \left(\phi/c\right)^2}{2} \right) = -\frac{\partial}{\partial x}(\phi u) \qquad 3.2$$

representing the time rate of the sum of kinetic and potential energy. The integration of (3.2) in a cyclic domain (or in one wavelength) leads its r.h.s to zero.

The substitution of a solution $e^{[i(kx-\sigma t)]}$ in the simplified model results in the dispersion relation:

$$\sigma = \pm ck \qquad 3.3$$

where k is the wavenumber and σ is the frequency. They are related to the wavelength L *and* period P by $k = 2\pi/L$ and $\sigma = 2\pi/P$, respectively.

b. The simple model in finite difference

The numerical scheme implemented to solve (3.1) follows the Lax-Wendroff principle (HOFFMAN, 1992). In order to be sure that the reduction on the amplitude of some frequencies (or modes) is due to the filter, the numerical scheme was slightly modified to an unstable scheme. It is a two-step scheme method proposed as follows:

first step

$$u_{j+1/2}^{n+1/2} = u_{j+1/2}^{n} - \frac{\Delta t}{2\Delta x}\left(\phi_{j+1}^{n} - \phi_{j}^{n}\right) \qquad 3.4\text{-a}$$

$$\phi_{j}^{n+1/2} = \phi_{j}^{n} - c^2 \frac{\Delta t}{2\Delta x}\left(u_{j+1/2}^{n} - u_{j-1/2}^{n}\right) \qquad 3.4\text{-b}$$

final step

$$u_{j+1/2}^{n+1} = u_{j+1/2}^{n} - \frac{\Delta t}{\Delta x}\left(\phi_{j+1}^{n+1/2} - \phi_{j}^{n+1/2}\right) \qquad 3.5\text{-a}$$

$$\phi_{j}^{n+1} = \phi_{j}^{n} - c^2 \frac{\Delta t}{\Delta x}\left(u_{j+1/2}^{n+1/2} - u_{j-1/2}^{n+1/2}\right) \qquad 3.5\text{-b}$$

where the subscripts stand the spatial grid-point and the superscripts the time-step.

The computational instability can be determined substituting the solution

$$\begin{pmatrix} u_j^n \\ \phi_j^n \end{pmatrix} = \begin{pmatrix} \hat{u}^n \\ \hat{\phi}^n \end{pmatrix} e^{ikj\Delta x}$$

into (3.1). The result is

$$\begin{bmatrix} \hat{u}^{n+1} \\ \hat{\phi}^{n+1} \end{bmatrix} = \begin{bmatrix} 1+c_4 & -c_1 s \\ -c_2 s & 1+c_4 \end{bmatrix} \begin{bmatrix} \hat{u}^{n} \\ \hat{\phi}^{n} \end{bmatrix} \qquad 3.6$$

where

$$c_1 = \frac{\Delta t}{\Delta x}; \quad c_2 = c^2 \frac{\Delta t}{\Delta x}; \quad c_3 = c_1 c^2 \frac{\Delta t}{2};$$

$$c_4 = c_3 \frac{2}{\Delta x}\left[\cos(k\Delta x) - 1\right] \quad \text{and} \quad s = 2i\,\mathrm{sen}\left(\frac{k\Delta x}{2}\right)$$

After some manipulations one obtains the equation for amplification factor λ in the form:

$$\lambda^2 - 2(1+c_4)\lambda + c_4(2+c_4) - c_1 c_2 s^2 + 1 = 0 \qquad 3.7$$

whose solutions are

$$\lambda = \left[1 + \left(c\frac{\Delta t}{\Delta x}\right)^2 \left[\cos(k\Delta x) - 1\right]\right] \pm \left[2c\frac{\Delta t}{\Delta x} sin\left(\frac{k\Delta x}{2}\right)i\right] \qquad 3.8$$

Fig.1 presents the amplify factor λ as a function of $c\Delta t/\Delta x$ for the most unstable wavelength, namely, $2\Delta x$. The numerical scheme proposed is unconditionally unstable, since $|\lambda| \geq 1$, as is the property required for this discussion.

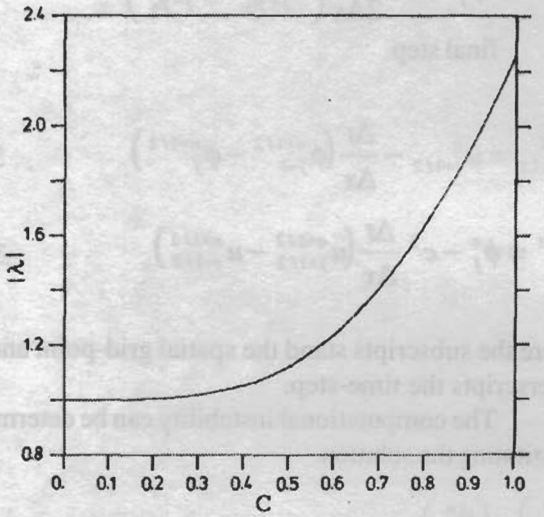

Fig 1 - the amplification factor l for the wavelength 2Δx in the numerical solution of the gravity wave model.

c. The digital filter applied to the simple model

The effect of the cutoff frequency imposed by the DF on the discretized gravity wave is examined in the following. The domain is constituted by 32 points with spatial resolution $\Delta x = 10^4 m$ The time-step is 1.2 s, and $H = 10^4 m$. These values result in $c\Delta t/\Delta x \approx 0.04$, and $|\lambda| \approx 1$ for all wavelengths. The integration performed in this study is 6000 time-steps and the amplitude amplification during this period is insignificant.

Boundary values are necessary in the computation of the spatial derivatives. The cyclic boundary condition is suitable in experiment concerning the behavior of wavemodes amplitudes, and will be used here.

The initial condition for the geopotential given by the following series

$$\phi_j = \frac{a_0}{2} + \sum_{k=1}^{16} \left[a_k \cos(k\omega x_j) + b_k \operatorname{sen}(k\omega x_j) \right] \qquad 3.9$$

and for the velocity

$$u_j^0 = 0, \qquad j = 1,2,...,32$$

with

$$x_j = j\Delta x \quad , \omega = \frac{2\pi}{32\Delta x} \, , \; a_k = b_k = \sqrt{2}/2, \text{ and } a_0 = 2$$

The simulated geopotential field is decomposed at each time-step into 16 spatial modes with wavelengths 32 Δx/k, k=1, 2,...,16 (formulation presented in Appendix). From this decomposition one obtain initially for each mode ϕ_k the amplitude $c_k = \sqrt{a_k^2 + b_k^2} = 1$ for all k, and kinetic energy equal to zero. In the forthcoming time-steps, due to the linearity of the problem, the c_k decreases until zero, when the kinetic energy reaches its maximum, and afterwards increases to achieve again the value 1. The gravity wave model during the whole integration produces this seesaw behavior with the total energy being conserved according to (3.2). The time required for one mode to return its amplitude to the value $c_k = 1$ represents its half-period of oscillation (from the maximum to the minimum). The relationship between frequency and wavelength follows the dispersion equation.

The frequency obtained by accompanying the oscillation of the c_k value is plotted at Fig. 2 for each numerical and analytical mode. It can be noted the error introduced by the discretization increases with the frequency (or decreases with wavelength). The shorter waves are the poorest simulated by the finite difference model, as should be expected (Haltiner and Williams 1980).

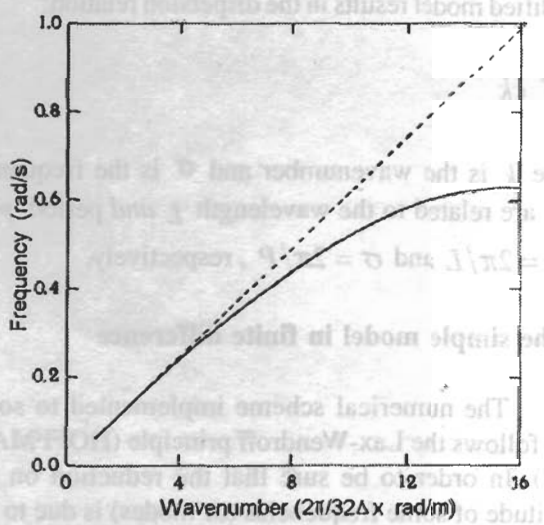

Fig.2 – Analytic (broken line) and numerical (continuous line) frequencies for the simple gravity-wave model, as a function of the wavenumber

The effect of the cutoff period on the filtered initial condition is now examined. After integrating the model for 6000 time-steps with a cutoff frequency in the DF, the model is integrated again with the filtered initial condition corresponding to the initial time-step 3000. As pointed above, before the use of the DF on the initial condition, the amplitude of each mode oscillates between 0 and 1. The maximum amplitude c_k for each mode during the integration starting with the filtered initial condition is displayed at Fig. 3. This procedure is carried out for the cutoff frequencies $2\pi/84\Delta t$, $2\pi/118\Delta t$, $2\pi/218\Delta t$, $2\pi/427\Delta t$, and $2\pi/849\Delta t$ which are equivalent according to the numerical dispersion relation (presented at Fig. 2) to the wavelength $2\Delta x$, $4\Delta x$, $8\Delta x$, $16\Delta x$ and $32\Delta x$ respectively. Note that the filter reduces the amplitude in about 50% of the applied cutoff frequency, more than 90% of higher frequencies, and preserves the amplitude of smaller frequencies. The Gibbs phenomenon also is well controlled by the Lanczos window.

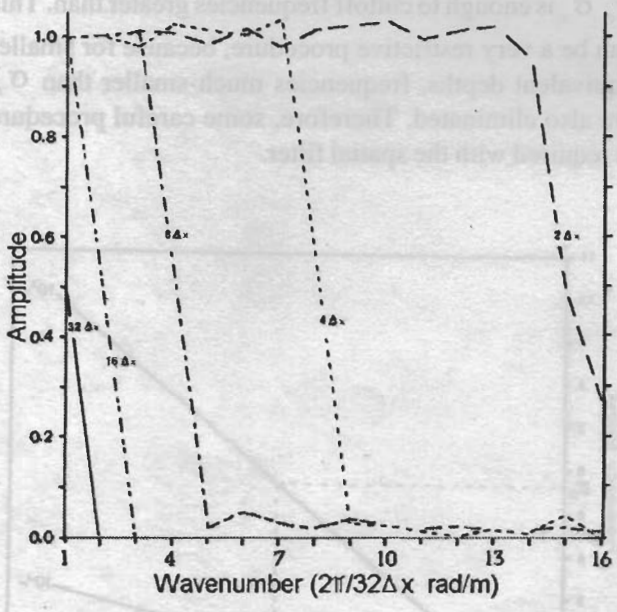

Fig.3 – Maximum amplitude of each wavelength after integrating the gravity-wave model with filtered initial condition and Lanczos window.

d. The assimilation of a simple function

The effect of the nudging in this simple problem is now examined. Consider the time weight presented in Section (2.b), equation (2.9), and a $16\Delta x$ wavelength mode for the geopotential given by

$$\phi(x) = sin\, k\,\frac{2\pi}{32\Delta x}\,x \quad , \text{with } k = 2$$

The first possibility is to assimilate only the geopotential ϕ and to let u be computed by its prognostic equation without any nudging. For initial condition u and ϕ are both set to zero. As soon ϕ evolves imposed by the nudging, a divergence (convergence) is generated where $\phi > 0$ ($\phi < 0$). The wind responds to the pressure gradient and takes out mass from regions with $\phi > 0$ and put on $\phi < 0$ (a typical behavior of gravity waves). While the nudging is growing, the removal of mass can not be enough to suppress the increase of the ϕ wave.

Fig. (4a) illustrates the time evolution (full line) of ϕ at the point j=16. The nudging process is dominant until the integration time of 4500 s, forcing ϕ to that imposed by the assimilated function. In response to the pressure gradient, the divergence and convergence of mass increase. The potential and kinetic energies integrated for whole domain are presented in Fig. 4.b and 4.c, respectively. The kinetic energy experiments a fantastic enhancement until the time-step 4500 because the nudging maintains the pressure gradient and does not allow the removal of mass, which would decrease the pressure gradient. As soon the nudging relaxes the kinetic energy decreases and the removal of mass is far strong yielding the potential energy to very high values. The same experiment is repeated by adding a nudging term in equation (3.1) imposing $u = 0$ in the velocity equation, and the results is presented also in Fig. 4 by dotted line. Note that the excessive increase of kinetic energy in the beginning and its posterior transformation into potential described in the previous experiment are now suppressed.

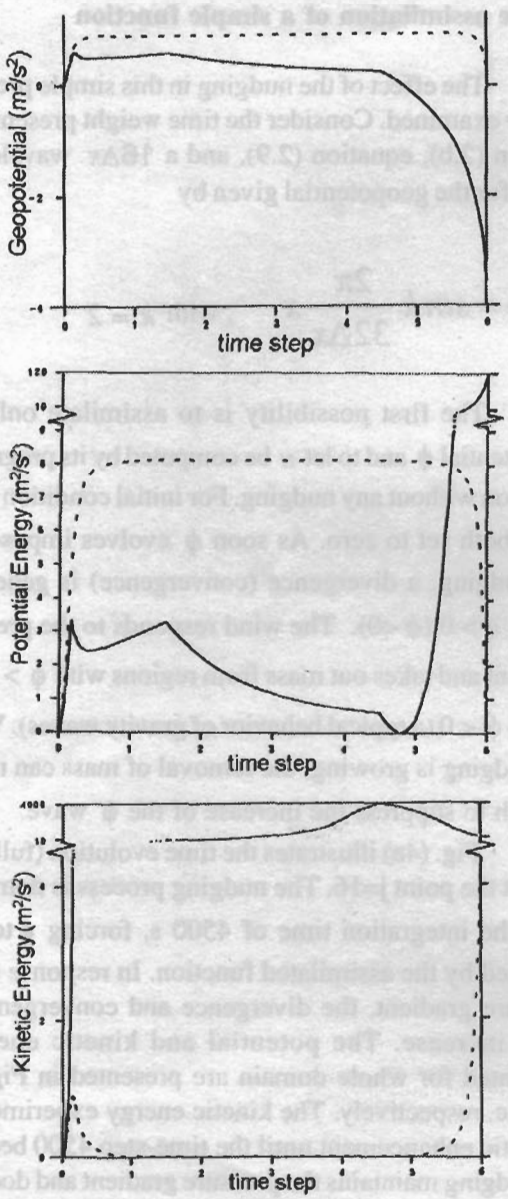

Fig. 4 - Time series of experiments nudging only (full line) and u (broken line) for (a) the geopotential integrated spatially and at point j = 16; (b) potential energy; and (c) kinetic energy. Time step is divided by 1000.

Conversely, the nudging of the variable u without any nudging of ϕ will increase the potential energy during the nudging process and the undesirable enhancement of total energy, noted in the first experiment, will also take place.

Although these results are obvious, they illustrate efficiently that the nudging of all prognostic variables can be conducted with relatively high nudging coefficients, but some care is necessary when one prognostic variable has no nudging term. In this case, the nudging weight must be small to avoid the excessive increase of potential or kinetic energy.

e. The simultaneous application of the filter and nudging schemes

Since the filter acts on the time series eliminating waves below a cutoff frequency, it becomes inefficient on a variable whose nudging term mask the oscillation. This happens because the method forces the variable to a certain prescribed value at each time-step.

In the simple problem studied, there is only one equivalent depth and the elimination of frequencies greater than σ_c is equivalent to cut off wavenumber greater than a certain value (k_c) This can be easily carried out by the use of a spatial filter, without needs for application of the DF, during the integration of the model. However, a problem with several equivalent depths, as in the case of an atmospheric model, this is not enough to eliminate all the wavenumber greater than k_c for smaller equivalent depths, as can be seen in Fig. 5, obtained from (3.4). Conversely, a spatial filter eliminating wavenumber $k > k_c$ σ_c is enough to cuttoff frequencies greater than. This can be a very restrictive procedure, because for smaller equivalent depths, frequencies much smaller than σ_c are also eliminated. Therefore, some careful procedure is required with the spatial filter.

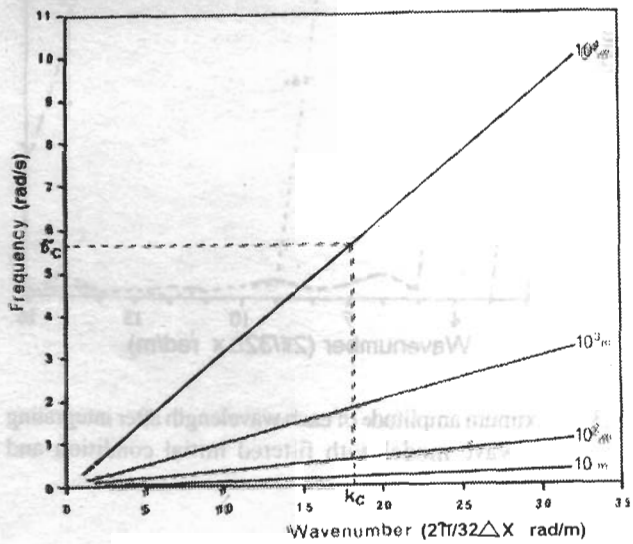

Fig. 5 - The dispersion relationship between the wavenumber k and the frequency σ, for the equivalent depth H.

An alternative approach, which will be examined in the following, is to apply the nudging only within the first half of the integrating period. In our gravity wave model, the time nudging coefficient is given by (2.9) with the time window 2T referring to 6000 time-steps, except that the coefficient is set zero for time-steps greater than 3000. It is then allowed the free modes to oscillate according to its dynamic, so the filter is able to eliminate the high frequencies left after the nudging be applied. Fig. 6 presents the result of an experiment with initial condition u and ϕ both set to zero, and the assimilated function (3.9) constituted by 16 modes with each amplitude equal to 1. The cutoff frequencies correspond to the wavelengths $2\Delta x$, $4\Delta x$, $8\Delta x$, $16\Delta x$ and $32\Delta x$ This figure shows that the filter reduces only about 50% of the frequency amplitude greater than the cutoff value. Also the undesirable Gibbs phenomenon is noticeable, and the Lanczos window was unable to control efficiently.

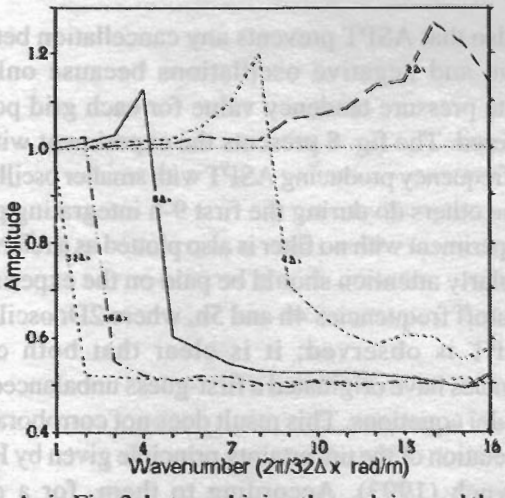

Fig. 6 – As in Fig. 3, but combining the nudging and the digital filter techniques.

However the Gibbs phenomenon is less pronounced with smaller cutoff frequencies, and in atmospheric numerical models short waves are well controlled by numerical artifices (horizontal diffusion). These arguments encourage the implementation of the approach in a complex atmospheric model, as will be discussed in the next section.

4. Application to a Primitive Equation Numerical Model

This section aims to investigate the combined use of DF and nudging to initialize a primitive equation numerical model. Although in the simple model studied above the Gibbs phenomenon was not controlled, the possibility of numerical artifices, like horizontal diffusion, in reducing or eliminating this harmful result in a complex numerical model is investigated.

a) The model description

The limited area numerical model (LAM) used here is a flux-form primitive equation grid point regional model developed at Numerical Prediction Division of Japan meteorological Agency and described in Nagata and Ogura (1991). The numerical code is constituted by 14 vertically layers in sigma coordinate, horizontal domain of 73 and 55 grid points in the east and north directions, respectively, in a Mercator projection. The grid distance on the map is 104.125 km true at 30° latitude. The boundary-layer processes are evaluated using the level 2-closure model (MELLOR and YAMADA 1974), and the surface fluxes are calculated by the similarity theory with the universal functions of Businger et al. (1971). The precipitation processes consider the grid scale condensation and Kuo scheme for the cumulus convection (KUO, 1965) with modifications suggested by Geleyn (1985). The sea surface temperature, constant during the integration, is obtained from a monthly average.

b) The case study

The case chosen to illustrate the method is a cyclone developing on South Atlantic at 31 December 1979. The 2.5° spatial resolution NCEP reanalysis at every 6 hour interpolated to the LAM domain are used as initial and lateral boundary conditions to the simulations, and also as assimilating nudged data during the filtering stage. Fig. 7 shows the mean sea level pressure, at interval of 12 h, beginning at 1200 UTC 31 Dec 1979. The cyclone deepens about 9 hPa/24h and moves northeastwards. The strong pressure gradient on the southwestern flank of the cyclone constitutes its remarkable feature because it was responsible for a long fetch with surface wind generating significant sea wave activity reaching the Uruguay and southern Brazilian Coasts. Although no ocean wave data is available to show its strength, the media reported an unusual wave heights and damages near the Southern Brazilian coast connected with this meteorological event around 32° S – 53° W.

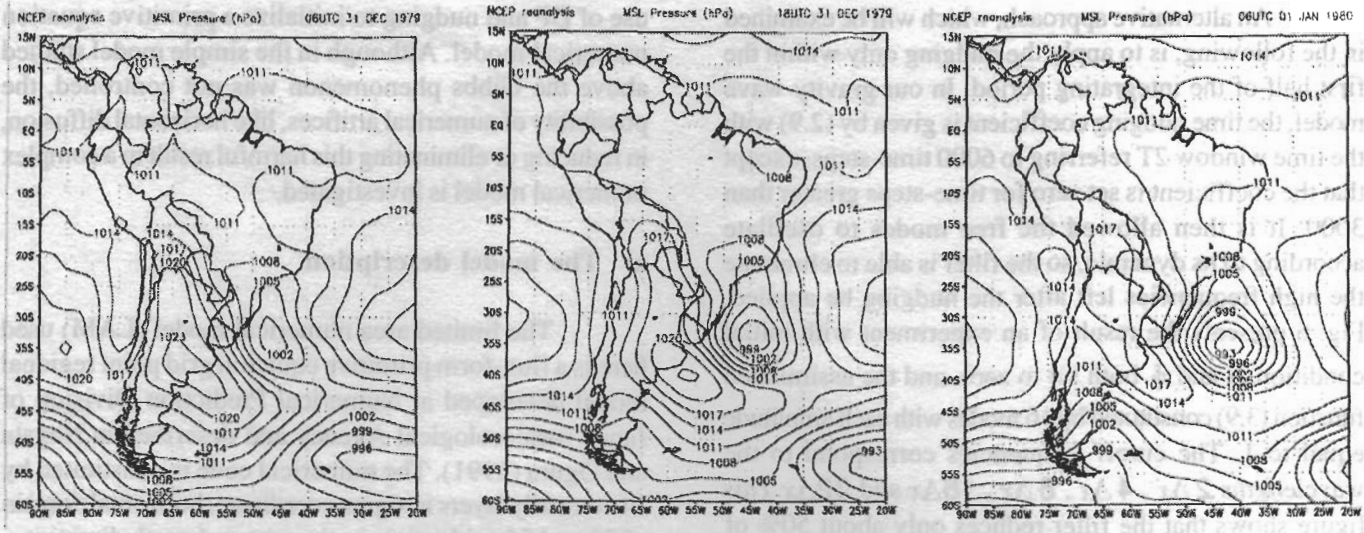

Fig. 7 – Mean Sea level pressure provided by the reanalysis of NCEP for 31 December 1979 at (a) 0600 UTC; (b) 1800 UTC; and (c) 0600 UTC 01 January 1980.

c) Sensitivity to the cutoff frequencies

These experiments use the initial condition at 1800 UTC 31 December 1979 obtained with cutoff frequencies of 1h, 2h, 3h, 4h and 5 h applied in a 12-h period of integration. In order to examine if the high frequency oscillation is actually eliminated by the filter, the absolute surface pressure tendency (ASPT) index proposed by Lynch and Huang (1992) was adopted. It is defined by

$$\text{ASPT} = \frac{1}{N}\sum_{i=1}^{N} \left| P_{s_i}^{n+1} - P_{s_i}^{n} \right| \Big/ \left(t^{n+1} - t^{n}\right)$$

where N is the grid point quantity, and $n+1$ and n refers to the time-step, and i to the grid point. This index is most suitable for this kind of analysis since it is able to capture all time oscillations present in the atmosphere.

Note also that ASPT prevents any cancellation between positive and negative oscillations because only the absolute pressure tendency value for each grid point is considered. The fig. 8 presents the experiment with 3-h cutoff frequency producing ASPT with smaller oscillations than the others do during the first 9-h integrating period (the experiment with no filter is also plotted as a reference). Particularly attention should be paid on the experiments with cutoff frequencies 4h and 5h, where 2Dt oscillation in ASPT is observed; it is clear that both cutoff frequencies have originated a first-guess unbalanced with the model equations. This result does not corroborate the interpretation of the uncertainty principle given by Huang and Lynch (1993). According to them, for a cutoff frequency corresponding to X hours the minimum time span is X/2 hours. Our result indicates that at least a time span of 4X is required to provide balanced initial conditions.

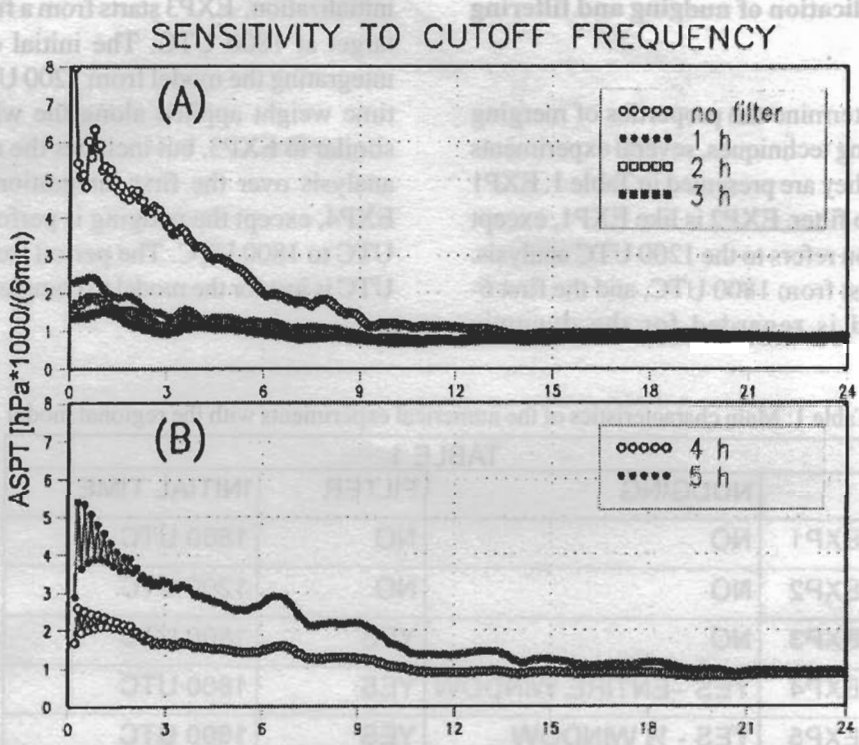

Fig. 8 – Absolute surface pressure tendency integrated over the domain as a function of time with initial conditions obtained for the cutoff frequencies (A) no filter, 1, 2 and 3 hours; (B) 4 and 5 hours.

d) Sensitivity to the nudging constant

Typical values for the nudging coefficients found in the literature are 7 x 10^{-5} s^{-1} (BAO and ERRICO 1997) and 2 ´ 10^{-4} s^{-1} (STAUFFER and SEAMAN 1990). In the present research values of 1.3 x 10^{-3} s^{-1}, 3.3 x10^{-4} s^{-1}, and 3.3 x 10^{-6} s^{-1} were tested in three experiments with no initialization. In the filtering stage, the initial condition is the analysis at 1200 UTC 31 December 1979 and the 1800 UTC analysis is nudged. Figure 9 shows ASPT as a function of time obtained with the integration starting at 1800 UTC. The three experiments evidence the needs for some kind of initialization. From FT = 3 h to FT = 9h the time weight is maximum and the noise clearly decreases gradually. After FT = 9h, the model is left oscillating by its own dynamics. There is a more pronounced adjustment in experiments with larger nudging coefficients. The value 1.3 x 10^{-3} s^{-1} for the nudging coefficient is adopted in this research because the ASPT seems to stay at acceptable values.

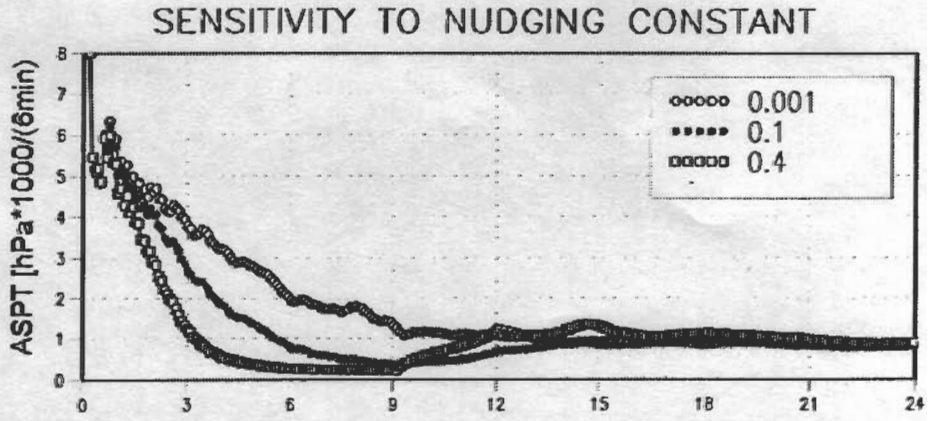

Fig. 9 – As in figure 8, but for several nudging coefficients without any initialization.

e) Simultaneous application of nudging and filtering techniques

In order to determine the properties of merging the nudging and filtering techniques, several experiments have been designed. They are presented in Table 1. EXP1 has no nudging and no filter. EXP2 is like EXP1, except that the initial condition refers to the 1200 UTC analysis. The result is shown just from 1800 UTC, and the first 6-h integrating period is regarded for the dynamic initialization. EXP3 starts from a filtered initial condition target at 1800 UTC. The initial condition is obtained integrating the model from 1200 UTC to 2400 UTC with time weight applied along the whole period. EXP4 is similar to EXP3, but includes the nudging of 1800 UTC analysis over the first integration stage. EXP5 is like EXP4, except the nudging is performed only from 1200 UTC to 1800 UTC. The period from 1800 UTC to 2400 UTC is just for the model to complete the filtering method.

Table 1: Main characteristics of the numerical experiments with the regional model

TABLE 1.			
	NUDGING	FILTER	INITIAL TIME
EXP1	NO	NO	1800 UTC
EXP2	NO	NO	1200 UTC
EXP3	NO	YES	1800 UTC
EXP4	YES –ENTIRE WINDOW	YES	1800 UTC
EXP5	YES - ½ WINDOW	YES	1800 UTC

Figure 10 presents the ASPT over the domain for a 24-h. A comparison among EXP1, EXP2 and EXP3 enables to discuss the effect of DF and model dumping. Without any initialization, the ASPT is very high in the beginning of the integration and takes about 9 h to achieve a stable stage with small variations. The dynamic initialization in EXP2 decreases ASPT, but presents some evidence that an additional period of 3 to 6-h of integration is necessary to reach the desirable stage. EXP3 shows the DF effect; it presents the ASPT substantially smaller than EXP1 and EXP2 during all 24-h period of integration. Although EXP3 exhibits a small $2\Delta t$ variation during the first 30 minutes, in general it seems to have less variations than the others experiments.

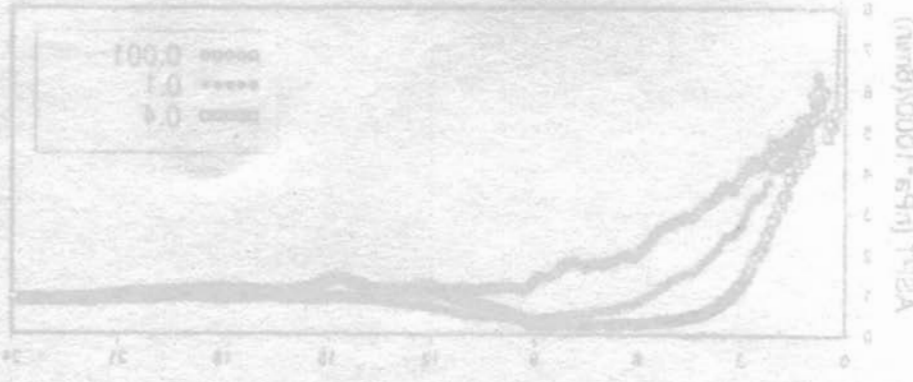

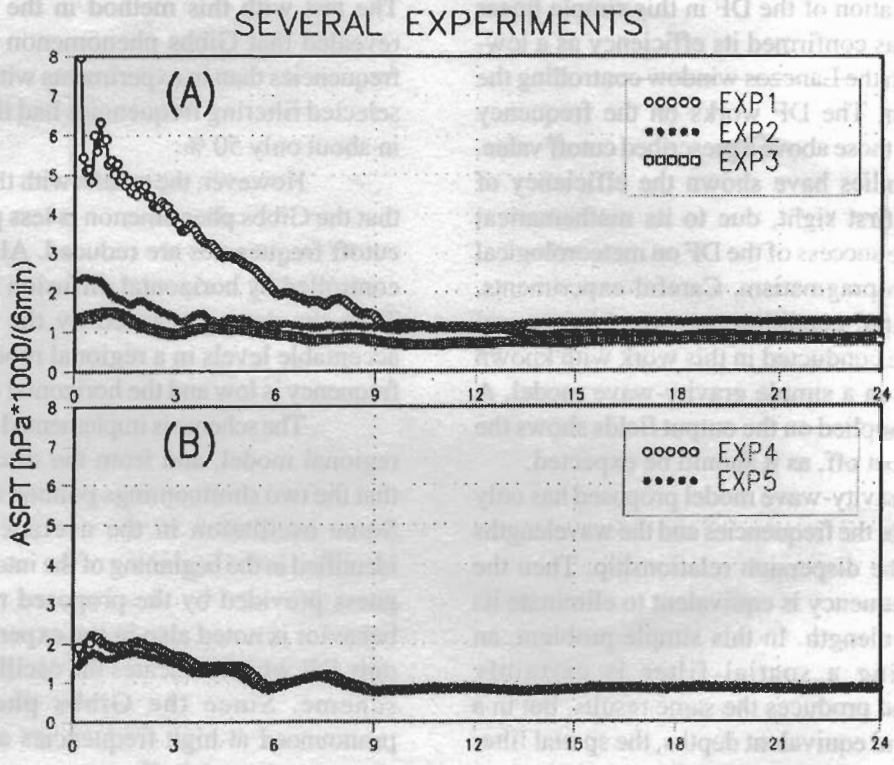

Fig. 10- As in figure 8, but for EXP1 (without nudging and initialization), EXP2 (like EXP1, but with dynamic initialization), EXP3 (no nudging and with DF), EXP4 (with both nudging and DF, applied over all time window), and EXP5 (like EXP4, but nudging only in the first half time window).

A comparison between EXP3 and EXP4 reveals that the nudging increases ASPT. The reduction of the assimilation time window, as depicted by the EXP5 in the same figure, decreases ASPT to almost the same level of the experiment with no nudging (EXP3).

Although no experiment with ASPT uniform has been identified, the proposed form of merging DF and nudging presents better performance than other experiments studied here. However, to access the success of the nudging is far more difficulty. At a first sight it seems that to show how close the assimilation come to the target analysis would be enough, but this is inappropriate because the approximation is controlled by the nudging coefficients. Then, in this research only the impact of the assimilation on the forecast was considered.

A comparison of MSLP (mean sea level pressure) and winds between EXP3 and EXP5 reveals the former develops a low pressure about 2hPa deeper at FT = 24 h, although such difference is not present in the initial condition. The EXP3 winds is stronger in all levels, mainly at surface (about 10 %). The NCEP reanalysis at 1800 UTC shows a weaker wind than that provided by the initialization of EXP3, and that seems the reason of EXP5 to present smaller wind. Although the nudged reanalysis accuracy can be argued, the nudging accomplishes its task, i.e., approximating the initial condition to the nudged field, as evidenced by EXP5.

5. SUMMARY AND CONCLUSIONS

A procedure to obtain a first-guess suitable for a regional model is proposed. In this method, the initialization technique by digital filter (DF) is implemented in a primitive equation regional model in conjunction with the nudging scheme to assimilate the global analysis. Both methods are known as very simple and efficient to be used in numerical models.

The scheme consists in integrating the model from an initial condition produced by a previous run, valid at 6-h before the first-guess target time. While a 12-h run is carried out to obtain the filtered field, the influence of a global analysis is incorporated by the nudging technique. Before we examine this idea on a regional primitive equation numerical model, a study of the characteristics and sensitivity of the nudging and DF methods separated and together is carried out on a linear gravity-wave model.

The application of the DF in this simple linear numerical model has confirmed its efficiency as a low-band pass filter, with the Lanczos window controlling the Gibbs phenomenon. The DF works on the frequency domain eliminating those above a prescribed cutoff value. Whereas others studies have shown the efficiency of DF, it seems in a first sight, due to its mathematical formulation, that the success of the DF on meteorological models is based on pragmatism. Careful experiments, with prescribed initial condition composed by several spatial modes, were conducted in this work with known cut off frequencies in a simple gravity-wave model. A harmonic analysis applied on the output fields shows the frequencies being cut off, as it should be expected.

Since the gravity-wave model proposed has only one equivalent depth, the frequencies and the wavelengths are connected by the dispersion relationship. Then the elimination of a frequency is equivalent to eliminate its correspondent wavelength. In this simple problem, an initialization using a spatial filter is certainly straightforward, and produces the same results, but in a problem with several equivalent depths, the spatial filter may not be enough to eliminate high frequencies.

Tests with the gravity wave model are carried out assimilating the velocity u, the geopotential ϕ, and both. The discussion shows that it is harmful to assimilate only one variable, because the forcing term obstructs the free oscillation of the variable. A gravity wave is characterized by alternating periods of conversion of kinetic into potential energy and vice-versa, so that the total energy is conserved. The forcing term does not allow the potential energy in case of assimilating ϕ (the kinetic energy, in case of u) decreases, because the pressure gradient (or the divergence and convergence) is maintained causing an increasing in kinetic energy (in potential energy). The final result is that after the assimilating nudging stage, the total energy increased to undesirable and dramatic levels. The assimilation of both prognostic variables (u and ϕ) eliminated this deficiency, and kept the total energy at acceptable levels.

The simultaneous application of the nudging and DF together in the simple model shows that the time oscillation is masked by the nudging, making the filter unable to work properly. In order to alleviate this deficiency, it is suggested to apply the nudging only on the first half of the total period so that the DF can feel the frequency to be cutoff in the second half time window. The test with this method in the gravity wave model revealed that Gibbs phenomenon is stronger at higher frequencies than in experiments without nudging, and the selected filtering frequencies had the amplitude reduced in about only 50 %.

However, the results with the simple model show that the Gibbs phenomenon is less pronounced when the cutoff frequencies are reduced. Also, shorter waves are controlled by horizontal diffusion in numerical models. Then the damage caused by the nudging can stay at acceptable levels in a regional model provide the cutoff frequency is low and the horizontal diffusion is sufficient.

The scheme is implemented in a primitive equation regional model, and from the discussion it is apparent that the two shortcomings pointed out are not so evident. Some oscillation in the average surface pressure is identified in the beginning of the integration using the first-guess provided by the proposed method, but a similar behavior is noted also in the experiment with the use of only DF, which indicates the oscillation is not due to the scheme. Since the Gibbs phenomenon is more pronounced at high frequencies as the simple test has shown, its harmful effect seems to be well controlled by the numerical diffusion of the primitive equation model.

APPENDIX

Decomposition of a Discrete Function

Consider a discrete sequence $\{f_n\}$, n=0,1, ..., m, representing (m+1) values in a ordinate x at the location $\{x_n\}$ The distance between two consecutive locations is Δx, and m is an odd number.

The sequence can be written as a sum of (m+1)/2 modes:

$$f(x) = \frac{a_0}{2} + \sum_{k=1}^{(m+1)/2} \left[a_k \cos(k\omega x) + b_k \operatorname{sen}(k\omega x) \right]$$

where

$$\omega = \frac{2\pi}{(m+1)\Delta x}$$

$$a_0 = \frac{2}{(m+1)} \sum_{n=0}^{m} f_n$$

$$a_k = \frac{2}{(m+1)} \sum_{n=0}^{m} f_n \cos(k\omega n\Delta x)$$

$$k = 1, \ldots, \frac{m+1}{2} - 1$$

$$b_k = \frac{2}{(m+1)} \sum_{n=0}^{m} f_n sin(k\omega n\Delta x)$$

$$a_k = \frac{1}{(m+1)} \sum_{n=0}^{m} f_n \cos(k\omega n\Delta x)$$

These results follows from

$$2\cos k\omega x_n = e^{ik\omega x_n} + e^{-ik\omega x_n}$$

$$2isink\omega x_n = e^{ik\omega x_n} - e^{-ik\omega x_n}$$

and from the orthogonality relations:

$$\sum_{n=0}^{m} e^{ik\omega x_n} = \begin{cases} m+1, & if\ k = 0, or\ k = m+1, or\ k = -(m+1); \\ 0, & otherwise \end{cases}$$

6. REFERENCES

BAO, J. W.; ERRICO, R. M., An adjoint examination of a nudging method data assimilation. **Mon. Wea. Rew.**, v.125, p.1355-1373, 1997.

BAER, F.; J.TRIBBIA, On complete filtering of gravity modes through non-linear initialization, **Mon. Wea. Rew.**, v.105, p.1536-1539, 1977.

BUSINGER, J. A., J. C. WYNGAARD, Y. IZUMI, AND E. F. BRADLEY, Flux-profile relationships in the atmospheric surface layer. **J. Atmos. Sci.**, v.28, p.181-189, 1971.

DALEY , R., Normal mode initialization. **Rev. Geo. Space Phys.** , v.19, p.450-468, 1981.

DOBLAS-REYES, F. J.; DÉQUÉ, M.,A flexible bandpass filter design procedure applied to midlatitude intraseasonal variability. **Mon. Wea. Rew.** , v.126, p.3326-3335, 1998.

FILLION, L.; MITCHELL, H. L.; RITCHIE, H.; STANIFORTH, A. The impact of a digital filter finalization technique in a global data assimilation system. **Tellus.** v.47A, p.304-323., 1995.

GELEYN, J. F., On a simple, parameter-free partition between moistening and precipitation in the Kuo scheme. **Mon. Wea. Rev.** , v.113, p.405-407, 1985.

GUSTAFSSON, N., Use of a digital filter as a weak constraint in variational data assimilation. Variational assimilation, with special emphasis on three dimensional aspects. ECMWF Seminar, p.327-338, 1992.

HALTINER, G. J.; WILLIAMS, R. T., **Numerical** prediction and dynamic meteorology. New York. John Wiley & Sons, 477 p. 1980.

HAMMING, R.W., Digital filters. Prentice-Hall International, 284 p. 1989.

HOFFMAN, J. D., Numerical methods for engineers and scientists. Mc Graw-Hill, 704 p. 1992.

HOKE, J. E.; ANTHES, R. A., The initialization of numerical models by dynamic initialization technique. **Mon. Wea. Rev.**, v.104, p.1551-1556, 1976.

HUANG, X. Y.; LYNCH, P. Diabatic Digital-filtering initialization: application to the HIRLAM model. **Mon. Wea. Rev.**, v.123, p.589-603. 1993:

KUO, H. L., On formation and intensification of tropical cyclones through latent heat release by cumulus convection. **J. Atmos. Sci.**, v.22, p.40-63, 1965.

KUO, Y. H.; GUO, Y. R.; WESTWATER, E. R. Assimilation of precipitable water measurements into a mesoscale numerical model. **Mon. Wea. Rev.**, v.121, p.12115-1238, 1993.

LYNCH, P.; HUANG, X. Y. Initialization of the HIRLAM model using a digital filter. **Mon. Wea. Rev.**, v.120, p.1019-1034, 1992.

MACHENHAUER, B., On the dynamics of gravity oscillations in a shallow water model with applications to normal mode initialization. **Contrib. Atmos. Phys.**, v.50, p.253-271, 1977.

MELLOR, G. L.; YAMADA, T. A hierachy of turbulence closure models for planetary boundary layers. **J. Atmos. Sci.**, v.31, p.1791-1806, 1974.

NAGATA, M.; OGURA, Y. A modeling case of interaction between heavy precipitation and a low-level jet over Japan in the Baiu season. **Mon. Wea. Rev.**, v.119, p.1309-1336, 1991.

STAUFFER, D. R.; SEAMAN, N. L. Use of four-dimensional data assimilation in a limited-area mesoscale model. Part I: Experiments with synoptic-scale data. **Mon. Wea. Rev.** , v.118, 1250-1277, 1990.